Ferroelectrics

Effect of Temperature and Frequency on Dielectric Properties of Aurivillius Type $Sr_{0.9}Pb_{0.1}Bi_{2-x}La_xNb_2O_9$ Ferroelectric Ceramics

Sameer Jain [a]; A. K. Jha [a]
[a] Dept. of Applied Physics, Delhi College of Engineering, Delhi, India

PLEASE SCROLL DOWN FOR ARTICLE

Taylor & Francis
Taylor & Francis Group

Effect of Temperature and Frequency on Dielectric Properties of Aurivillius Type $Sr_{0.9}Pb_{0.1}Bi_{2-x}La_xNb_2O_9$ Ferroelectric Ceramics

SAMEER JAIN[*] AND A. K. JHA

Dept. of Applied Physics, Delhi College of Engineering, Delhi–110042, India

In the present work, keeping a small quantity of lead (10 atomic %) at Sr site, the contents of La have been varied at Bi site to study the behavior of SBN. Samples of compositions $Sr_{0.9}Pb_{0.1}Bi_{2-x}La_xNb_2O_9$ (with x = 0.0 to 0.2) were prepared by solid state reaction method. X ray diffraction analysis reveals the formation of single phase perovskite structure. Although the perovskite structure of SBN is retained, slight changes in the lattice parameters are observed. Tetragonal strain is observed to decrease in the La doped samples. Dielectric constant and dielectric loss have been measured as a function of temperature(300–800 K) and frequency (100 Hz–100 kHz). It is observed that there is an overall decrease in dielectric constant with increasing lanthanum content. It is also observed that dielectric loss decreases with increasing amount of La content. Curie temperature is observed to decrease from 440°C for pure SBN to 230°C for La (x = 0.20) doped sample. The variation of conductivity with temperature in these samples is also reported.

Introduction

$SrBi_2Nb_2O_9$ (SBN) is one of the most promising fatigue resistant ferroelectric ceramic well known for its excellent fatigue characteristics, high Curie temperature, high remanant polarization, low coercive field and low leakage current [1–3]. These ceramics have attracted the attention of researchers due to their potential applications in non–volatile random access memories (NvRAM), high capacitance capacitors, etc. Bismuth layered Aurivillius type compounds have a general formula $[Bi_2O_2]^{2+}[A_{n-1}B_n\ O_{3n+1}]^{2-}$ consisting of peroviskite $[A_{n-1}B_n\ O_{3n+1}]^{2-}$ layers sandwiched between $[Bi_2O_2]^{2+}$ layers. Here A can be Ba^{2+}, Sr^{2+}, Pb^{2+} etc. and B can be Nb^{5+}, Ta^{5+}, etc [4]. These ceramics are very sensitive to the compositional variations. Changing the stoichiometry or doping with various elements remarkably influences crystal structure and ferroelectric properties. In bismuth layer structured ferroelectrics, bismuth layer influences the structural, electrical and ferroelectric properties of these ceramics [4–6]. In bismuth layer structures stoichiometry of the system is difficult to maintain as bismuth oxide has high vapor pressure and is evaporated off at higher temperatures leaving behind cationic and anionic vacancies [4]. These vacancies are responsible for distorted unit cells structure which results in high ferroelectric response

---

along a–b plane and increased lattice strain along c-axis. Due to stoichiometric disparity bismuth oxide layer may induces space charge [7]. Bismuth oxide layer is paraelectric in nature while peroveskite unit cell is ferroelectric [8]. Hence it is interesting to study the effect of addition of La at Bi site with a small amount (10 at %) of lead at Sr site. These effects have been studied in the present work and are reported here.

Experimental

Polycrystalline strontium bismuth niobate ceramic samples of compositions $Sr_{0.9}Pb_{0.1}$-$Bi_{2-x}La_xNb_2O_9$ (x = 0.0 to 0.2 in steps of 0.05) were prepared by solid-state reaction method. $SrCO_3$, PbO, Bi_2O_3, La_2O_3, Nb_2O_5 (all from Aldrich of 99.9% purity) were taken in stoichoimetric proportions, thoroughly mixed, ground and passed through sieve of appropriate size. Mixtures were calcined at 900° C in air for 2 hours. The calcined specimens were mixed with appropriate quantity of polyvinyl alcohol and then molded into disc shape pellets by applying a pressure of 300 MPa. Pellets were finally sintered at 1200°C for 2 hrs. X–ray diffraction data were collected for these samples on a Philips X–ray diffractometer using CuK_α radiations (range $10° \leq 2\theta \leq 70°$). Silver paste was used on the pellets to form electrodes. The dielectric parameters were measured at 100 KHz on an Agilent 4284A LCR meter at oscillation amplitude of 1 volt.

Result and Discussions

1. Micro Structural Studies

Figure 1 shows the XRD patterns of some of the studied samples. The position and intensity of the peaks in X-ray diffractograms show the formation of single-phase perovskite orthorhombic structure in all the samples. A small variation in the position and intensity of the peaks is observed which is possibly due to the variations in the lattice parameters. It is
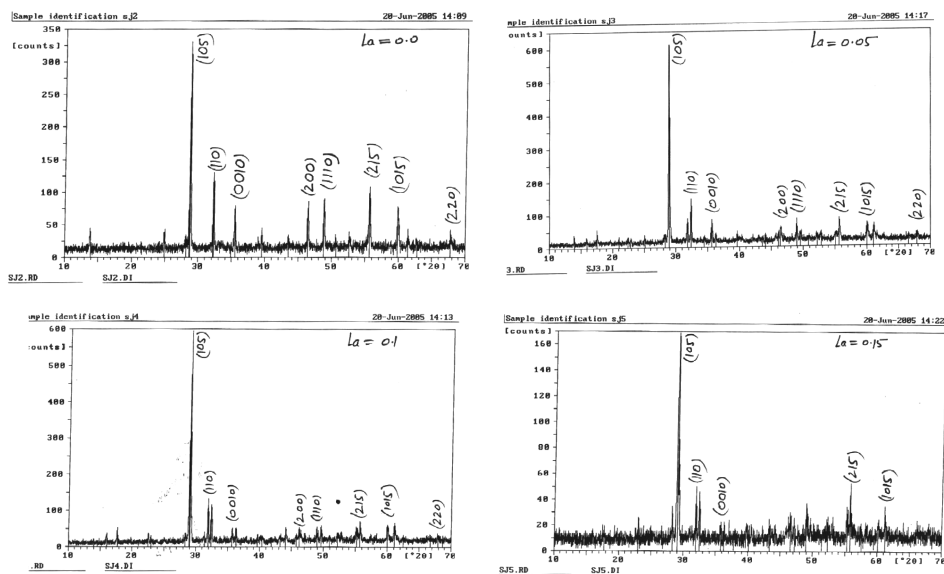

Figure 1. X-Ray diffractograms of samples $Sr_{0.9}Pb_{0.1}Bi_{2-x}La_xNb_2O_9$ (x = 0.0 to 0.2).

also observed that with increase in La content, the background noise increases, indicating a decrease in crystalline nature of the sample. The samples with x = 0.05 and 0.1 show high crystalline structure while x = 0.15 and 0.2 are less crystalline as evident from the disappearance of few peaks of low intensity.

The intensity of few peaks is observed to decrease with increase in La content indicating the decrease in perovskite phase in the sample. Lattice parameters have been calculated from the obtained d-values. La doped samples show very small changes in the lattice parameters. Tetragonal strain (c/a) of the samples was calculated using the obtained lattice parameters. Tetragonal strain of the studied samples shows an overall decrease with increasing La content.

2. Dielectric Studies with Temperature

Figure 2 shows dielectric constant as a function of temperature at 100 kHz. These observations have been plotted using microcal origin 6.1. Dielectric constant of pure SBN is more than Pb and La doped samples. Large number of vacancies in SBN at Bi sites are expected because of bismuth oxide evaporation at higher temperature during sintering process [9]. Replacement of Bi by La not only stabilizes the crystal structure but would also creates fewer vacancies at Bi site. This is possibly the cause for the lower dielectric constant of SPBLN than that of SBN. The value of dielectric constant has four-polarization contributions, namely: orientational polarization, ionic polarization, electronic polarization and space charge polarization [10,11]. The dielectric constant is observed to decrease with increasing La content. The dielectric constant of these samples is affected besides other factors by the evaporation of bismuth oxide during sample preparations. This results in space charge generation, which plays an important role in influencing dielectric response of the samples.

Figure 3 shows the variation of Curie temperature with increasing La content. The temperature at which the phase transition occurs corresponds to Curie temperature of the
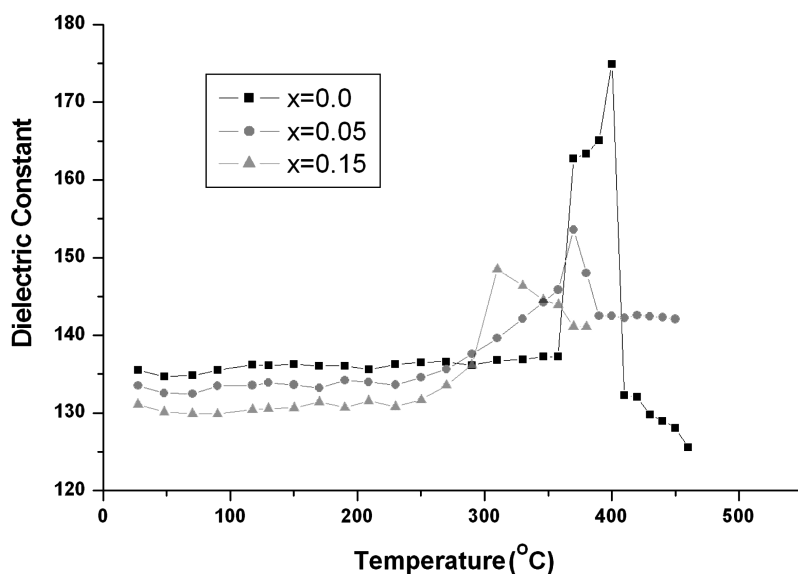

Figure 2. Dielectric const. vs Temp. of $Sr_{0.9}Pb_{0.1}Bi_{2-x}La_xNb_2O_9$ at 100 kHz. (See Color Plate VI)
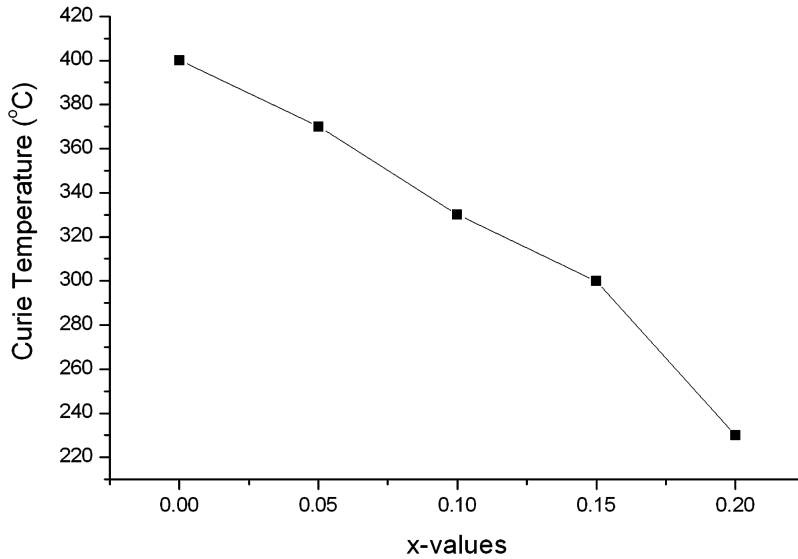
Figure 3. Curie temperature vs x- values in $Sr_{0.9}Pb_{0.1}Bi_{2-x}La_xNb_2O_9$.

sample. Curie temperature decreased from 400°C for La free sample to 230°C for La (x = 0.20) doped sample. A decreased tetragonal strain in La doped samples is attributed to be the cause for the decrease in Curie Temperature [6]. La doping reduces lattice parameters [13] and stabilizes the crystal structure. Reduced parameters are expected to show less ferroelectric behavior [14].

Figure 4 shows dielectric loss as a function of temperature measured at 100 kHz. The dielectric loss of SBN at Curie temperature is 1.39 and that of SPBLN (x = 0.20) at Curie temperature is 0.86. Dielectric loss increases with increase in temperature and the increase
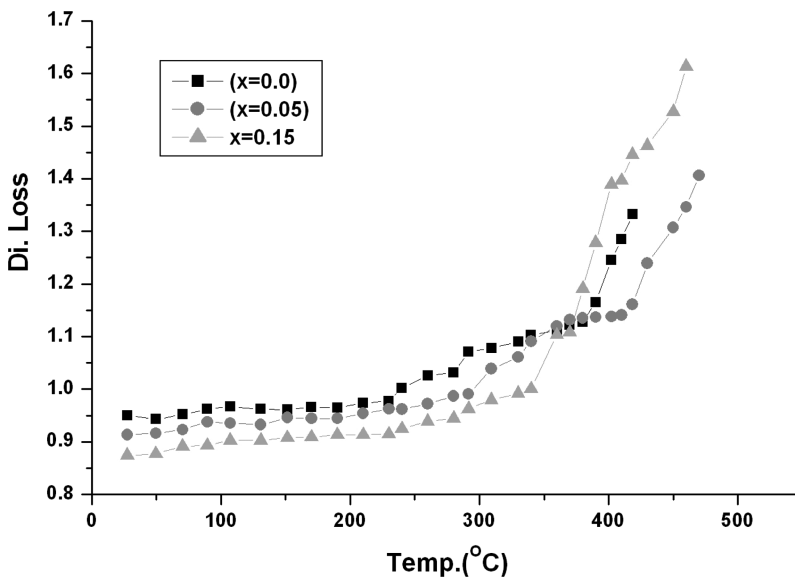

Figure 4. Dielectric loss vs x-values in $Sr_{0.9}Pb_{0.1}Bi_{2-x}La_xNb_2O_9$ at 100 kHz. (See Color Plate VII)
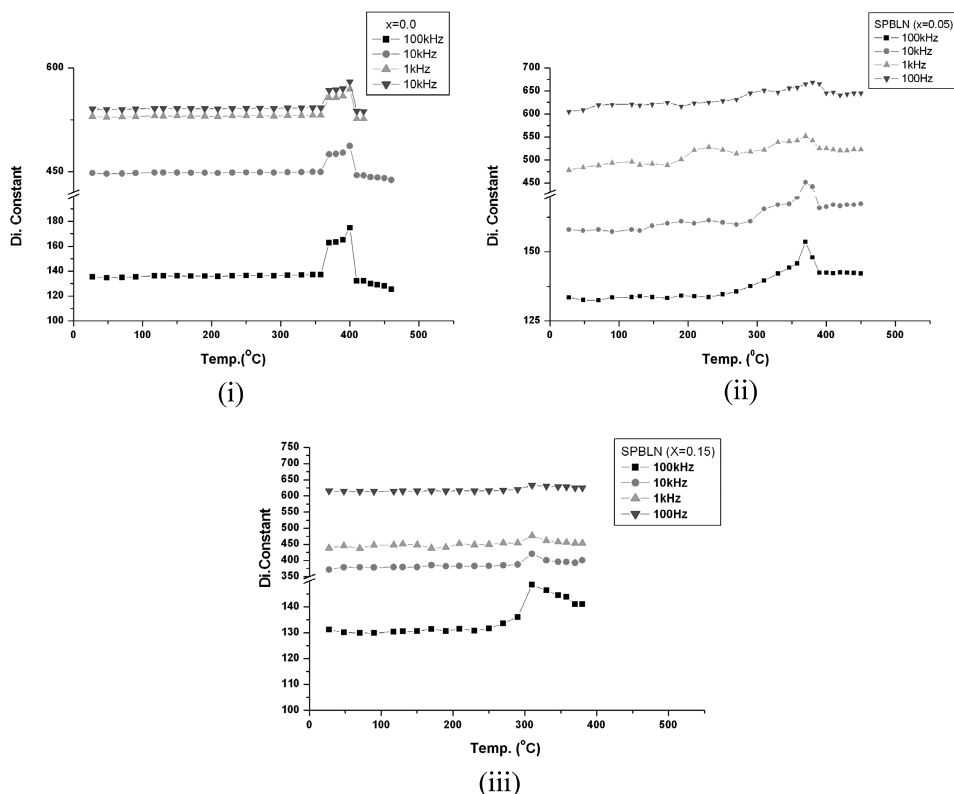
Figure 5. Dielectric const. vs Temp. of $Sr_{0.9}Pb_{0.1}Bi_{2-x}La_xNb_2O_9$. (x = 0.0, 0.05, 0.15) at different frequencies. (See Color Plate VIII)

is sharp at higher temperatures. This is possibly due to high concentration of charge carriers present in the sample at higher temperature. Similar observations have been made by others [4–6, 15, 16].

3. Dielectric Studies with Frequencies

Figure 5 shows the dielectric constant measured at frequencies 100 Hz, 1 kHz, 10 kHz, 100 kHz, as a function of temperature. The observations are similar to those reported in other systems [17–19]. The peak of the curves i.e. the maximum permitivity is observed to decrease with increasing frequency. As the frequency increases the maximum value of permitivity decreases and the overall nature approaches the normal relaxors behavior. These features are typical of a thermally activated Debye relaxation in these frequency regions. The subsequent monotonous increase of dielectric constant at higher temperature is due to the increase in conductivity [20, 21]. The apparent transition temperature remains the same at all the frequencies. The broadness of curve possibly arises due to heterogeneity present in the material. Increased permitivity at the higher temperature may be due to the mobile charge carriers, which may be related to the oxygen vacancies. The oxygen vacancies related polarization become more prominent at elevated temperature due to the increased density of oxygen vacancies [22]. Decrease in permitivity upon increasing the frequency indicates a large contribution due to space charge polarization in the doped samples.
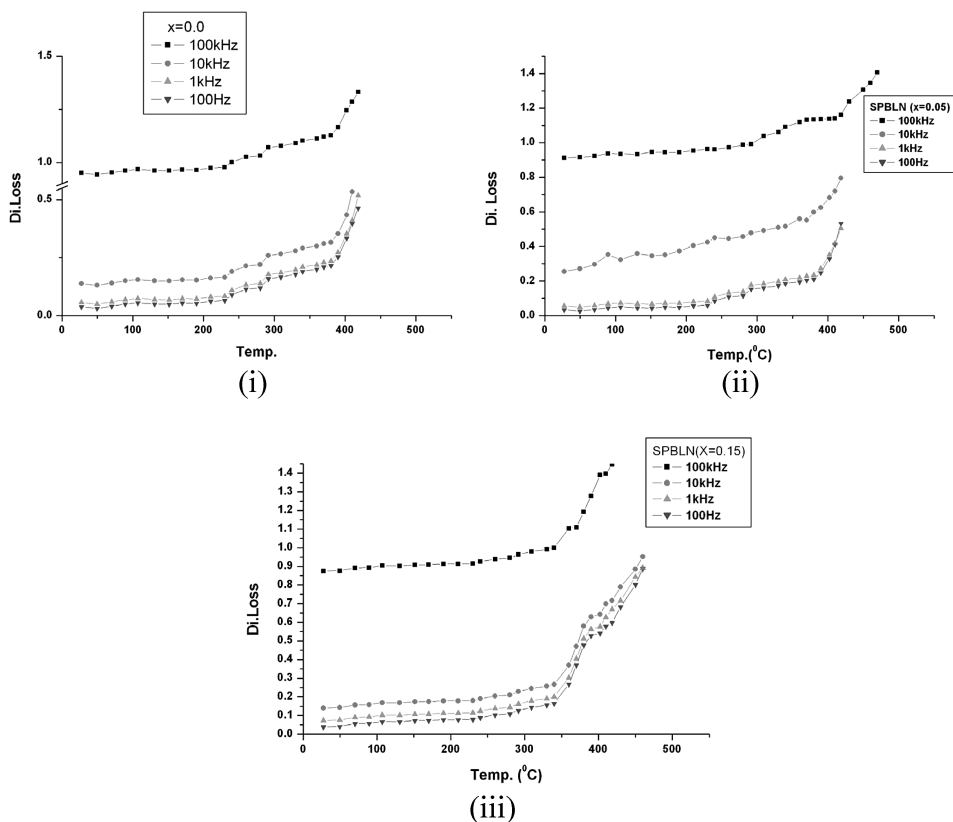
(i)

(ii)

(iii)

Figure 6. Dielectric loss vs Temp. of $Sr_{0.9}Pb_{0.1}Bi_{2-x}La_xNb_2O_9$ ($x = 0.0, 0.05, 0.15$) at different frequencies. (See Color Plate IX)

Figure 6 shows the dielectric loss measured at frequencies 100 Hz, 1 kHz, 10 kHz and 100 kHz, as a function of temperature. Dielectric loss increases with increase in frequency. The loss is caused by space charge and domain wall relaxation. It is reasonable to assume that the space charge is the main reason for a change in dielectric loss as the frequency increases.

4. Dielectric Studies with La Content

Figure 7 shows the variation of Dielectric Constant and Dielectric Loss as a function of La content. Although, there is not a monotonic variation but an overall decrease in dielectric constant with increasing La content is observed. It is also observed that the dielectric loss decreases continuously with increasing amount of La content.

5. A.C. Conductivity

A.C. conductivities of all the studied samples have been calculated using impedance data according to the relation:

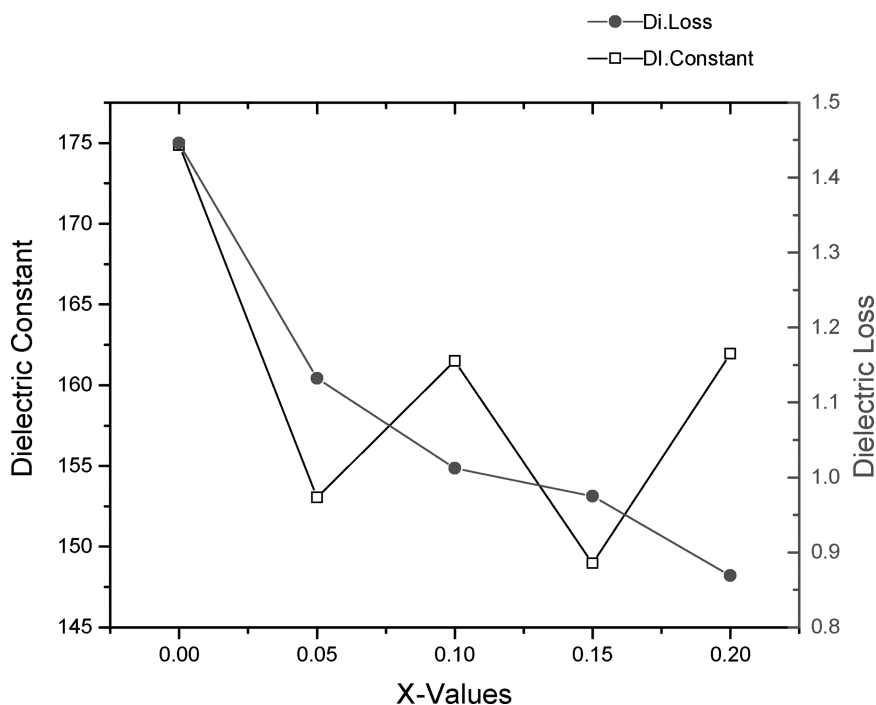$$\sigma_{a.c.} = 2\pi f \varepsilon_0 \varepsilon_r D$$

Figure 7. Dielectric constant & dielectric loss vs x-values in$Sr_{0.9}Pb_{0.1}Bi_{2-x}La_xNb_2O_9$. (See Color Plate X)

where f is the frequency permittivity, ε_0 is the permitivity of free space, $\varepsilon_r$is the dielectric constant and D is the dielectric loss. Figure 8 shows the variation of a.c conductivity with La content. It is observed that a.c. conductivity decreases with increasing value of La. The electronic configuration of Bi (83) is $[Xe]^{54}4f^{14}$ $5d^{10}6s^26p^3$and that of La is $[Xe]^{54}5d^3$.

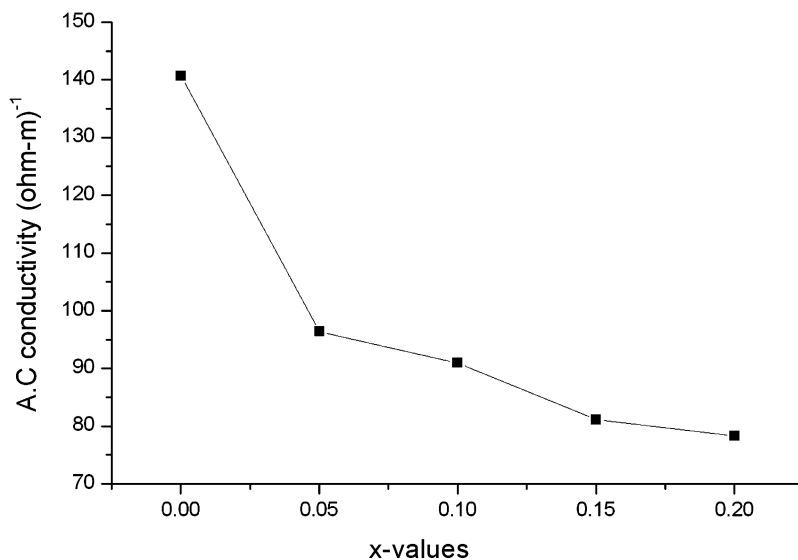**Figure 8.** A.C. conductivity vs x-values in $Sr_{0.9}Pb_{0.1}Bi_{2-x}La_xNb_2O_9$.

La^{3+}ion has no outer electron in contrast to a Bi^{3+}ion which has a lone pair of 6s electrons, This causes less hybridization with 2p orbital of oxygen and should lead to wider band gap [23]. This may be the cause for the observed decrease in a.c. conductivity.

Conclusions

It is concluded from the present work that La doping in $Sr_{0.9}Pb_{0.1}Bi_{2-x}La_xNb_2O_9$ at Bi site reduces tetragonal strain considerably. Due to the reduced tetragonal strain the Curie temperature and dielectric loss reduces. Dielectric constant decreases with increasing frequency while dielectric loss increases with increasing frequency. Also Dielectric constant decreases in La doped samples in comparison to La free samples. A.C. conductivity is also observed to decrease with increasing La content of the samples.

Acknowledgment

References

1. B. Aurivillivas, *Arki Kemi* **1**, 463 (1949); **1**, 499 (1949); **2**, 579 (1950).
2. C. A. P. de aranzo, and J. F. Scott, *Science* **246**, 1400 (1989).
3. AI Kingon, Current opinion in solid state and material science in 1999, Elsevier, p. 39.
4. Vaibhav Srivastava, A. K. Jha, and R. G. Mendiratta, *Solid-state communications* **133**, 125–129 (2005).
5. Vaibhav Srivastava, A. K. Jha, and R. G. Mendiratta, Materials Letters (In Press).
6. Vaibhav Srivastava, A. K. Jha, and R. G. Mendiratta, *Physica B* **371/2**, 337 (2006).
7. Y. Noguchi, H. Shimizu, M. Miyayama, K. Oikawa, and T. Kamiyama, *Jap. Journal of Applied Physics* **40**, 5812 (2001).
8. H. Irie, M. Miyayama, and K. Kudo, *Jour. of applied Physics* **90**, 4089 (2001).
9. Haifeng, Yinyin Lin, and Ting-Ao-Tang, *Solid State Communications* **135**, 304 (2005).
10. Relva C. Buchanan, Ceremics material for electronics, Marcell Dekker Inc., New York 1986.
11. Indrani Coondoo, A .K. Jha, and S. K. Agaarwal, Ceramics International (In Press).
12. Y. Wu, M. J. Forbess, S. Seraji; S. J. Limmer T. P. Chon, and G. Cao. *Jour of applied Physics* **89**, 5647 (2001).
13. Ferroelectric materials and their application by Yuhuan H. Xu, *Elsevier Sc. Publishers B.V. P.* **165** (1991).
14. Ferroelectric crystals by F Jonea, *G Shirane Perganon Press Oxford* **10**, 276 (1962).
15. Y. Shimakawa, Y. Kubo, Y. Tauchi, H. Asno, T. Kamiyama, F. Izumi, and Z. Hiroi, *Appl. Physics letter.* **79**, 2791–2793 (2001).
16. Rizwana, G. S. Kumar, and P Sarah, Proceedings of XII NSFD, India, Nov-23-25, (2003).
17. E. C. Subbarao, *J. Phys. Chem. Solids.* **23**, 665–676 (1992).
18. P. Durain-Martin, A. Castro, P. millan, and B. Jimenez, *J. Mater. Res.* **13**(9), 2565–2571 (1998).
19. S. M. Zenetti., E. I. Santiago, L. O. S. Bulhoes, J. A. Varela, E. R. Leite, and E. Lonngo, *Mater. Letters* **57**, 2812–2816 (2003).
20. S. Ezhilvalava, J. M. Xue, and J. Wang, *Mater. Chem. and Phy.* **75**, 50–55 (2002).
21. O. Bidault, P. Goux, M. Kchikech, M. Bilkaourmi, and M. Maglione, *Phys. Rev. B* **49**, 7868 (1994).

22. Puja Goel and K. L. Yadav, *Physica B* **382**, 245–251 (2006).
23. Rizwana, G. S. Kumar, and P Sarah, *Indian J. Phy.* (in press).
24. Ferroelectrics Devices, K. Uchino, Marcell Dekker Inc., New York, p. 93 (2000).
25. Principles of electronics ceremics by R. C. Buchnan, Marcel Deckkar Inc. New York, pp. 38–39 (1991).
26. C. E. Land P Thacher, and G. H. Hartling, *Electropic Ceramics Advances in materials and Device Research* **4**, 137–233 (1974).